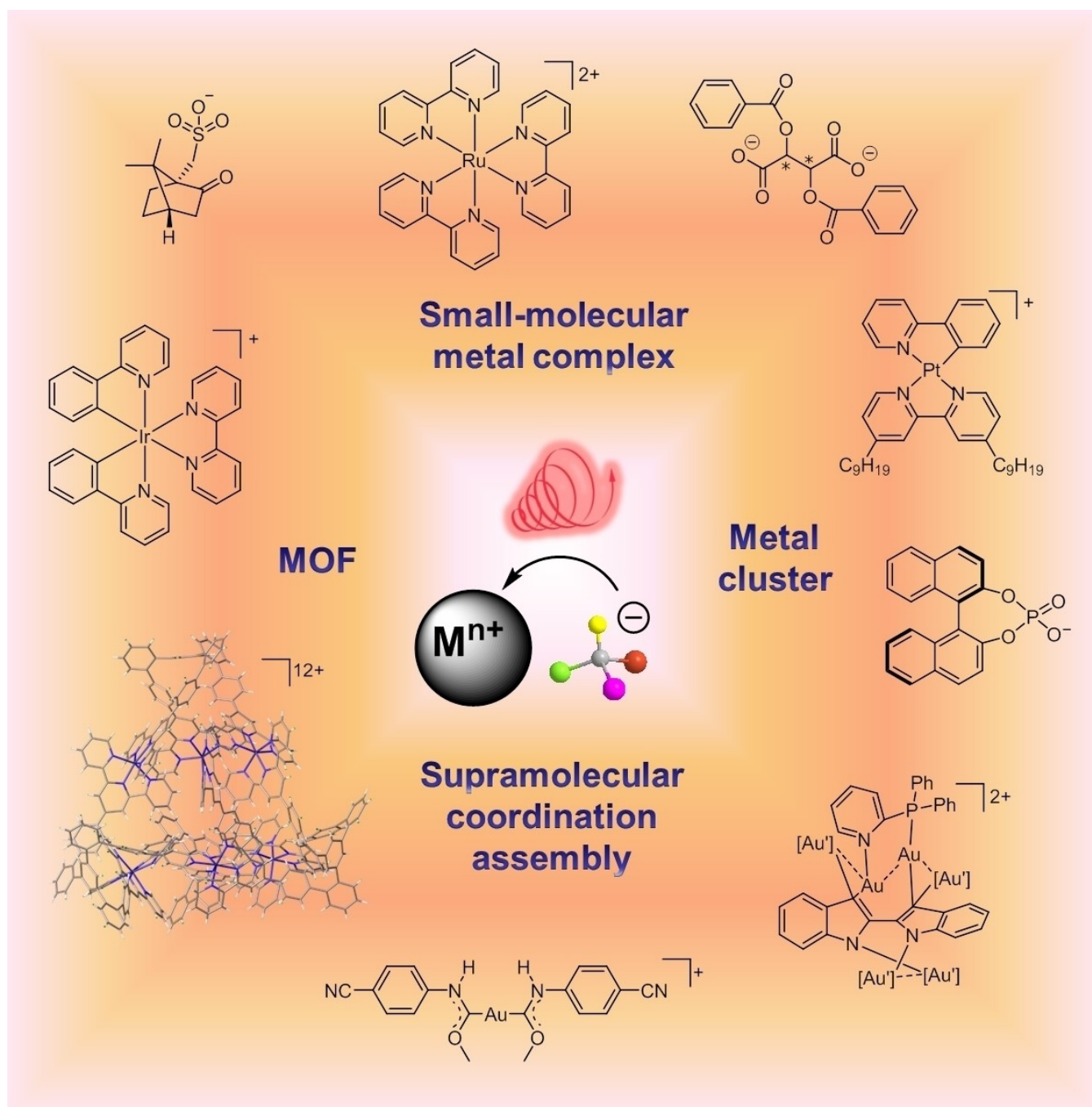


# Endowing Metal-Organic Coordination Materials with Chiroptical Activity by a Chiral Anion Strategy

Yuan-Yuan Zhao,<sup>[a, b]</sup> Zhong-Qiu Li,<sup>[a]</sup> Zhong-Liang Gong,<sup>[a]</sup> Stefan Bernhard,<sup>[c]</sup> and Yu-Wu Zhong<sup>\*[a, b]</sup>



Recently, chiral metal-organic coordination materials have emerged as promising candidates for a wide range of applications in chiroptoelectronics, chiral catalysis, and information encryption, etc. Notably, the chiroptical effect of coordination chromophores makes them appealing for applications such as photodetectors, OLEDs, 3D displays, and bioimaging. The direct synthesis of chiral coordination materials using chiral organic ligands or complexes with metal-centered chirality is very often tedious and costly. In the case of ionic coordination materials, the combination of chiral anions with cationic, achiral coordination compounds through noncovalent interactions may endow molecular materials with desirable chiroptical

properties. The use of such a simple chiral strategy has been proven effective in inducing promising circular dichroism and/or circularly polarized luminescence signals. This concept article mainly delves into the latest advances in exploring the efficacy of such a chiral anion strategy for transforming achiral coordination materials into chromophores with superb photo- or electro-chiroptical properties. In particular, ionic small-molecular metal complexes, metal clusters, coordination supramolecular assemblies, and metal-organic frameworks containing chiral anions are discussed. A perspective on the future opportunities on the preparation of chiroptical materials with the chiral anion strategy is also presented.

## 1. Introduction

Chirality is a fundamental attribute of nature and it is ubiquitous at various hierarchical levels, from the molecular to the macroscopic scale, of natural and synthetic objects. As an essential feature of nature, chirality plays an indispensable role across diverse fields, including pharmaceutics, industrial chemicals, biology, and materials science.<sup>[1]</sup> A pair of chiral enantiomeric molecules are characterized with identical molecular formulas and physicochemical properties and they form mirror images that do not superimpose. These molecules can contain one or more than one type of molecular chirality, including point, plane, axis, and helical chirality, etc.<sup>[2]</sup> Point chirality involves an asymmetric chiral carbon, to which four distinct types of atoms or groups are attached. Planar chirality arises when a molecule has two non-coplanar dissymmetric rings which cannot rotate easily around the chemical bond connecting them.<sup>[3]</sup> Axial chirality appears in a molecule that possesses an axis with a set of substituents, whose spatial arrangement does not superimpose with its mirror image.<sup>[4]</sup> Helical chirality refers to the phenomenon that the left- and right-handed helices cannot overlap due to their distinct rotation directions and it can be present either in molecules or assemblies.<sup>[5]</sup> When a molecule contains two or more chiral centers, diastereomers can be distinguished, which are stereoisomers but not mirror images of each other.

Currently, the development of chiral materials has drawn extensive attention due to their numerous potential applications in asymmetric synthesis, chiral sensing and recognition, light-emitting, and enantioseparation, etc.<sup>[6]</sup> In addition, the appealing

chiroptical properties of chiral chromophores have exhibited promising potentials in photodetectors, OLEDs, 3D displays, and bioimaging.<sup>[7,8]</sup> Circular dichroism (CD) and circularly polarized luminescence (CPL) are two distinctive optical characteristics of chiral materials, owing to their intrinsically noncentrosymmetric nature. CD signals are caused by the differential absorption of the right- and left-circularly polarized (RCP and LCP, respectively) light by a specific chiral material, reflecting the ground-state nature of the material. CPL is a chiral emission phenomenon from the excited states of emitters. The magnitude of CD can be quantified by the absorption dissymmetry factor  $g_{\text{abs}}$  (or  $g_{\text{CD}}$ ), as determined by Eq. (1):

$$g_{\text{abs}} = \frac{2(\varepsilon_L - \varepsilon_R)}{(\varepsilon_L + \varepsilon_R)} \quad (1)$$

where  $\varepsilon_R$  and  $\varepsilon_L$  stand for the molar absorption coefficients for the RCP and LCP light, respectively. The CPL property is typically evaluated by the luminescence dissymmetry factor  $g_{\text{lum}}$ , as defined by Eq. (2):

$$g_{\text{lum}} = \frac{2(I_L - I_R)}{(I_L + I_R)} \quad (2)$$

where  $I_L$  and  $I_R$  are emission intensity of left- and right-handed CPL (L-CPL and R-CPL) of a chiral emitter, respectively. The values of  $g_{\text{abs}}$  and  $g_{\text{lum}}$  are both in the range from  $-2$  to  $+2$ . In addition to the  $g_{\text{lum}}$  factor, the emission quantum yield  $\Phi$  is also an important parameter for the characterization of CPL materials. Currently, it remains a challenge to obtain materials with both high intrinsic  $g_{\text{lum}}$  and  $\Phi$ . A high  $g_{\text{lum}}$  needs a molecule with a small electric dipole moment  $\mu$ ; however, a large  $\mu$  is typically needed to obtain a high  $\Phi$ .<sup>[9]</sup>

Chiral emissive materials are typically prepared through one of the following methods. The most straightforward approach is by incorporating a suitable molecular chirality, e.g. point, plane, axis, or helical chirality, into the emissive materials by a covalent connection. In addition, the mirror symmetry breaking of a mixture of enantiomers offers a simple method to obtain chiral materials.<sup>[10]</sup> These chiral materials can display intrinsic chiroptical properties as discrete molecules, e.g. in dilute solutions, or varied luminescent and chiroptical properties upon assembly. Beyond single-component molecules, the co-assembly of two or more subcomponents provides a powerful means to obtain chiral emissive materials, which is sometimes accompanied by appeal-

[a] Y.-Y. Zhao, Dr. Z.-Q. Li, Dr. Z.-L. Gong, Prof. Y.-W. Zhong

Beijing National Laboratory for Molecular Sciences (BNLMS), CAS Key Laboratory of Photochemistry, CAS Research/Education Center for Excellence in Molecular Sciences

Institute of Chemistry, Chinese Academy of Sciences, Beijing 100190, China  
E-mail: zhongywu@iccas.ac.cn

[b] Y.-Y. Zhao, Prof. Y.-W. Zhong

School of Chemical Sciences  
University of Chinese Academy of Sciences, Beijing 100049, China

[c] Prof. S. Bernhard

Department of Chemistry  
Carnegie Mellon University, Pittsburgh, Pennsylvania 15213, United States of America

ing chirality amplification. The co-assembly method is advantageous in avoiding the sometimes tedious synthetic procedures and is able to generate color- and handedness-tunable chiral signals by regulating the assembly conditions. The presence of sufficient noncovalent interactions, such as host-guest interaction,<sup>[11]</sup> hydrogen bonding,<sup>[12]</sup> charge transfer interaction,<sup>[13]</sup> electrostatic interaction,<sup>[14]</sup>  $\pi$ - $\pi$  stacking interaction,<sup>[15]</sup> have been proven to be important in inducing efficient chirality transfer between different subcomponents.

To date, a large number of chiroptical materials have been developed, including small organic molecules, polymers, inorganic materials, or organic-inorganic hybrid materials.<sup>[7–15]</sup> Among them, metal-organic coordination materials including small molecular metal complexes, metal clusters, coordination polymers, and metal-organic frameworks (MOFs), have received considerable attention.<sup>[16]</sup> One representative example is chiral Eu(III) complexes, which are characterized with large  $g_{\text{lum}}$  values due to the unique electronically-forbidden yet magnetically-allowed f-f transitions.<sup>[17]</sup> Coordination materials possess appealing electronic and optical properties that can arise from the metal centers, the organic ligands, or as a result of the charge transfer among them. They are characterized with rich electrochemistry and photophysical properties.<sup>[18]</sup> They may adopt various molecular configurations depending on the metal-ligand coordination mode, such as linear, planar, tetrahedral, and octahedral configurations, which heavily influence their assembly behavior. Due to the strong spin-orbit coupling effect, metal

complexes often display triplet phosphorescence with relatively long excited-state lifetimes and high luminescence quantum yields. The combination of chirality and metal complexes is believed to create chiroptical materials with effective circularly polarized phosphorescence (CPP). However, the synthesis of enantiomerically pure metal complexes is not a trivial task and it is equally challenging for the development of chiral phosphorescent metal complexes with both high  $g_{\text{lum}}$  and  $\Phi$  values.

We present in this concept article the use of a simple chiral anion strategy to endow ionic coordination materials with chiroptical properties. It is noted that the chiral ion-pairing is a well-established method in asymmetric chemical synthesis, which involves the effective chirality transfer from an enantiomerically pure ionic species to a charged reaction substrate or intermediate.<sup>[19]</sup> In comparison, a similar chiral ion-pairing method in inducing chiroptical properties of ionic luminescent materials have been less developed. This method is effective for ionic materials, in which readily available chiral components are used as counter anions for the cationic, racemic luminophores.<sup>[20]</sup> The efficient electrostatic and hydrogen bonding interactions between the anionic and cationic components give rise to the desired chiroptical activity. This method is characterized with a simple synthesis procedure. Efficient CD and photo- and electro-CPL properties have been achieved using this method in a number of small-molecular metal complexes, metal clusters, coordination supramolecular assemblies, and MOFs, as is discussed below. In particular, the modulation of chiroptical



Yuan-Yuan Zhao received her B.S. degree from Zhengzhou University in 2021. She is currently a doctor graduate student at the Institute of Chemistry, Chinese Academy of Sciences (ICCAS) under the supervision of Prof. Yu-Wu Zhong. Her recent research focuses on luminescent organic-inorganic hybrid metal halides.



Zhong-Qiu Li received her B.S. degree from Nankai University in 2017 and Ph.D. degree from ICCAS under supervision of Prof. Yu-Wu Zhong in 2022. She is currently a postdoc associate in the Zhong's group at ICCAS. Her research interests focus on luminescent molecular materials and devices.



Zhong-Liang Gong obtained his Ph.D. degree from ICCAS under supervision of Prof. Yu-Wu Zhong in 2015. After that, he worked as an assistant professor in the Zhong's group at ICCAS from 2015 to 2020, and as an associate professor in the same group since 2020. His current interests mainly focus on synthesis and optoelectronic application of luminescent transitional metal complexes.



Yu-Wu Zhong obtained his Ph.D. degree in 2004 from Shanghai Institute of Organic Chemistry, Chinese Academy of Sciences. After working as a postdoctoral associate at the University of Tokyo (2004–2006) and Cornell University (2006–2009), respectively, he started his independent career from 2009 and worked to present as a full professor at ICCAS. His research interests include the syntheses of photofunctional and electrofunctional molecular materials and their applications in mixed-valence chemistry, electrochromism, organic nanophotonics, and perovskite solar cells.

properties through the use of different chiral anions is highlighted.

## 2. Chiroptically Active Coordination Materials

### 2.1. Small-Molecular Metal Complex

Chiral transition metal complexes (TMCs) have attracted intense recent attention due to their diverse coordination modes, rich excited-state properties, and high  $\Phi$  or  $g_{\text{lum}}$  values.<sup>[16,21]</sup> In particular, tris-bidentate octahedral Ru<sup>II</sup> and Ir<sup>III</sup> complexes are

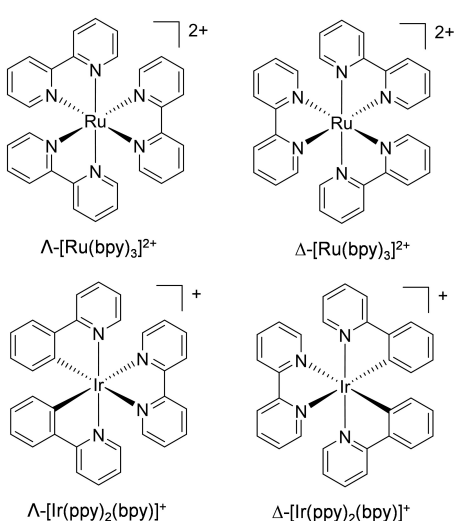


Figure 1. Chemical structures of representative chiral Ru<sup>II</sup> and Ir<sup>III</sup> complexes with metal-centered chirality. Counter anions are PF<sub>6</sub><sup>-</sup> if otherwise noted.

two classical and representative families of luminescent TMCs that have received wide applications.<sup>[22]</sup> These complexes are intrinsically chiral that can be distinguished by the  $\Lambda$  or  $\Delta$  metal-centered chirality, where the three bidentate ligands form a left or right helix, respectively, as represented by the classical complexes [Ru(bpy)<sub>3</sub>]<sup>2+</sup> (bpy = 2,2'-bipyridine) and [Ir(ppy)<sub>2</sub>(bpy)]<sup>+</sup> (ppy = 2-phenylpyridine) (Figure 1). Though the chemical structures of these chiral complexes look simple, it is rather difficult to obtain enantiomerically pure molecules of these complexes. It is very difficult to separate the  $\Lambda$  and  $\Delta$  enantiomers of these complexes by the direct resolution with chiral high-performance liquid chromatography (HPLC). One practical method is first to obtain a chiral intermediate containing two bidentate ligands, e.g. bpy or ppy, and another chiral organic ligand, followed by the reaction with the third bidentate ligand.<sup>[23]</sup> This method is however complicated and costly. The exploration of alternative approaches to decorate TMCs with chiral information and chiroptical properties is highly desired.

In conjunction with the development in CPL-active ionic molecular crystals consisting of organic cations of conjugated pyridinium derivatives and chiral organic anions,<sup>[20]</sup> Zhong and coworkers recently explored the possibility of endowing ionic TMCs (iTMCs) with CPL activity by using the chiral anion strategy. A series of diastereomeric Ir<sup>III</sup> and Ru<sup>II</sup> complexes with chiral (+) or (-)-camphorsulfonate anions (CSA<sup>-</sup>) have been prepared, without separating the  $\Lambda$  and  $\Delta$  enantiomers (Figure 2).<sup>[24]</sup> Though the solutions of these diastereomers are CPL-inactive, the microcrystals of these complexes are characterized with efficient CPPs with  $|g_{\text{lum}}|$  in the range of 0.5×10<sup>-2</sup> to 4.0×10<sup>-2</sup> and  $\Phi$  of 5%–85%. The microcrystals of the di-cationic Ru<sup>II</sup> complexes, Ru1((-)-CSA)<sub>2</sub> (Ru1 = [Ru(bpy)<sub>3</sub>]<sup>2+</sup>) and Ru2((-)-CSA)<sub>2</sub>, and the tri-cationic Ir<sup>III</sup> complex Ir4((-)-CSA)<sub>3</sub> show distinctly

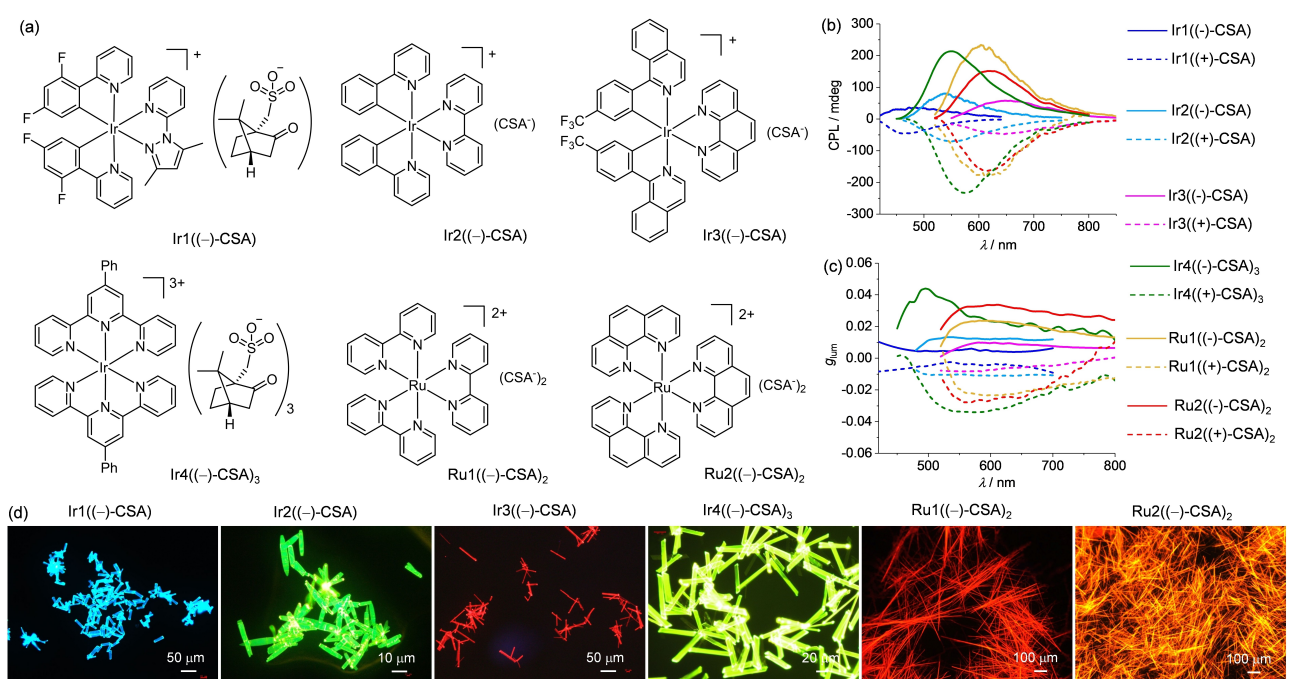


Figure 2. (a) Chemical structures of ionic complexes with chiral (-)-CSA<sup>-</sup>. (b,c) CPL and  $g_{\text{lum}}$  spectra and (d) fluorescence microscopy images of corresponding microcrystals. Reproduced with permission from Ref. [24]. Copyright: 2023, Science China Press.

higher  $|g_{\text{lum}}|$  than those of the other mono-cationic complexes (the structures are given in Figure 2a). This suggests that the increasing numbers of chiral anions are beneficial for improving the CPL property. The emission colors can be modulated by changing the structures of TMCs. Single crystal X-ray analysis suggests that multiple hydrogen bonding interactions are present between  $\text{CSA}^-$  and the achiral cationic metal components, which are believed important to promote the underlying chirality transfer process. When  $\text{CSA}^-$  with an opposite chirality is used, mirror-imaged CD and CPL signals associated with the low-energy metal-to-ligand charge-transfer (MLCT) transition are obtained.

In addition to the generation of circularly polarized photoluminescence, the above chiral anion strategy is also effective in producing circularly polarized electroluminescence (CPEL). Three pairs of iTMCs with  $\text{CSA}^-$ ,  $\text{Ir}5((\pm)\text{-CSA})$ ,  $\text{Ir}2((\pm)\text{-CSA})$ , and  $\text{Ru}1((\pm)\text{-CSA})_2$  have been used for this purpose (the structure of  $\text{Ir}5$  is given in Figure 3a and those of  $\text{Ir}2$  and  $\text{Ru}1$  are available in Figure 2a).<sup>[25]</sup> The solutions and spin-coated films of these diastereomeric complexes are essentially CPL-inactive. In contrast, using these complexes as the active layer, the light-emitting electrochemical cells (LEECs) with a sandwiched device structure of ITO/PEDOT:PSS/iTMCs/LiF/Al exhibit decent CPELs (Figure 3). The addition of the chiral ionic liquid  $(+/-)$ -1-butyl-3-methylimidazole camphorsulfonate  $((\pm)\text{-IL})$  into the active layer is found to distinctly improve the device performance and the electroluminescence dissymmetry factors ( $g_{\text{EL}}$ ). In particular, the device with 2/1  $\text{Ir}2((\text{-})\text{-CSA})/(\text{-})\text{-IL}$  gives  $g_{\text{EL}}$  of  $-2.3 \times 10^{-3}$  at 582 nm, maximum luminescence of  $12320 \text{ cd/m}^2$ , and external quantum efficiency (EQE) of 4.71 %. This work is interesting in that the CPEL of the LEEC device is significantly amplified with respect to the circularly polarized photoluminescence of the thin film. This is in stark contrast with common circularly polarized organic light-emitting diodes (CP-OLEDs) in which chirality diminishment is often observed for electrical devices with respect to corre-

sponding samples in solutions or films.<sup>[26]</sup> The electrically amplified CPELs in LEECs is attributed to the accumulated chiral  $\text{CSA}^-$  near the electrode upon applying the electric field, which facilitates the chirality transfer and amplification between chiral anions and TMCs.

The two works mentioned above show that the chiral anion strategy is feasible in producing both circularly polarized photo- and electroluminescence. The diastereomeric complexes with chiral counter anions are directly used in both cases. This avoids the difficulty in preparing the enantiomeric  $\Lambda/\Delta$  TMCs. However, the effectiveness of other chiral anions beyond  $\text{CSA}^-$  in inducing CPLs remains to be explored.

With the rapid development of supramolecular chemistry, chiral supramolecular self- or co-assembly systems have become a powerful method to prepare CPL materials with amplified  $g_{\text{lum}}$  and high  $\Phi$  through the formation of ordered molecular assemblies, in particular helical nanostructures.<sup>[27]</sup> In this context, the co-assembly of achiral materials with chiral anion inducers through intermolecular interactions provides a simple way for the generation and amplification of chirality.

You and coworkers reported a combined top-down and bottom-up method for the simultaneous amplification of  $\Phi$  and  $g_{\text{lum}}$  by the co-assembly strategy using an achiral square-planar  $\text{Pt}(\text{II})$  complex with chiral carboxylic anions (Figure 4).<sup>[28]</sup> They selected the  $\text{Pt}(\text{II})$  complex  $\text{PtN}^+$  cation to co-assemble with the enantiomeric  $(L/D)$ -dibenzoyl tartarate  $((L/D)\text{-BT})$ ,  $(L/D)$ -dipivaloyl tartarate  $((L/D)\text{-PT})$ , and  $(R/S)$ -tetrahydrofuran-2-carboxylate  $((R/S)\text{-TC})$  carboxylic anions with different charges and substituents to examine the relationship between chiral anions and chiroptical properties (the structures of these materials are given in Figure 4a and 4b). The assembly of  $\text{PtN}(\text{ClO}_4)$  without chiral anions affords spherical aggregates with no CPL activity. In contrast, helical fibrillar assemblies are obtained from  $\text{PtN}^+$  in the presence of  $(D)$ - or  $(L)$ -BT, showing efficient CPL with  $g_{\text{lum}}$  of 0.037 and  $-0.033$ , respectively at 570 nm. However, the uses of  $(L/D)$ -

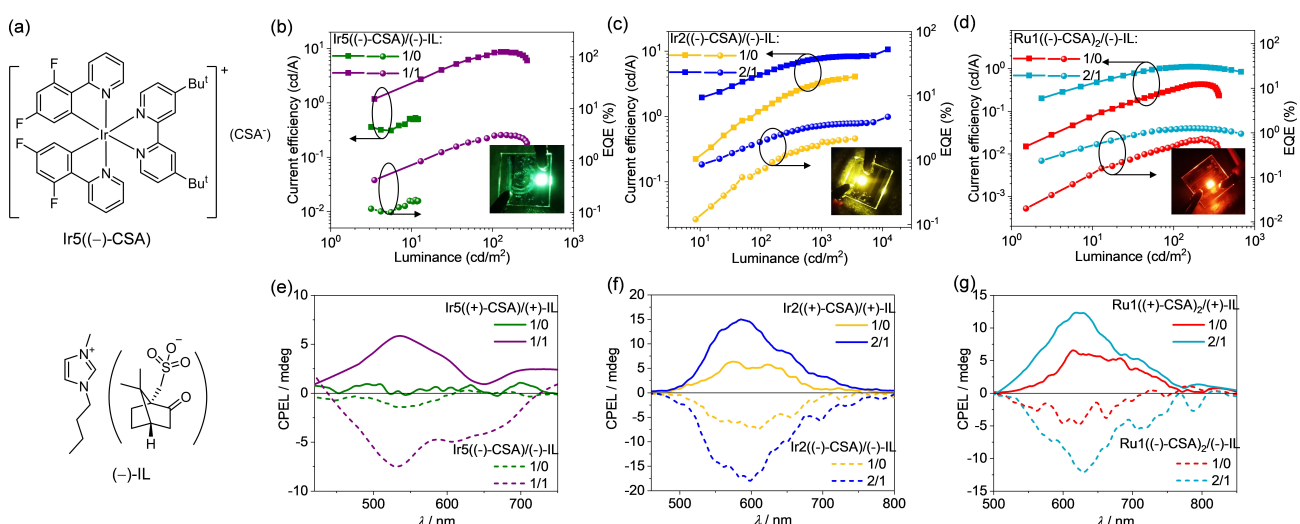


**Figure 3.** (a) Structures of  $\text{Ir}5((\text{-})\text{-CSA})$  and  $(\pm)\text{-IL}$ . (b-d) Current efficiency-luminance-EQE curves and (e-g) CPEL spectra of the LEEC devices with  $\text{Ir}5((\pm)\text{-CSA})$ ,  $\text{Ir}2((\pm)\text{-CSA})$ , and  $\text{Ru}1((\pm)\text{-CSA})_2$  in the absence or presence of chiral ILs (the molar ratios of iTMCs/IL are indicated). The insets of panel (b, c, d) display the images of corresponding LEECs in the presence of IL. The structures of  $\text{Ir}2$  and  $\text{Ru}1$  are available in Figure 2. Reproduced with permission from Ref. [25]. Copyright: 2023, Wiley-VCH.

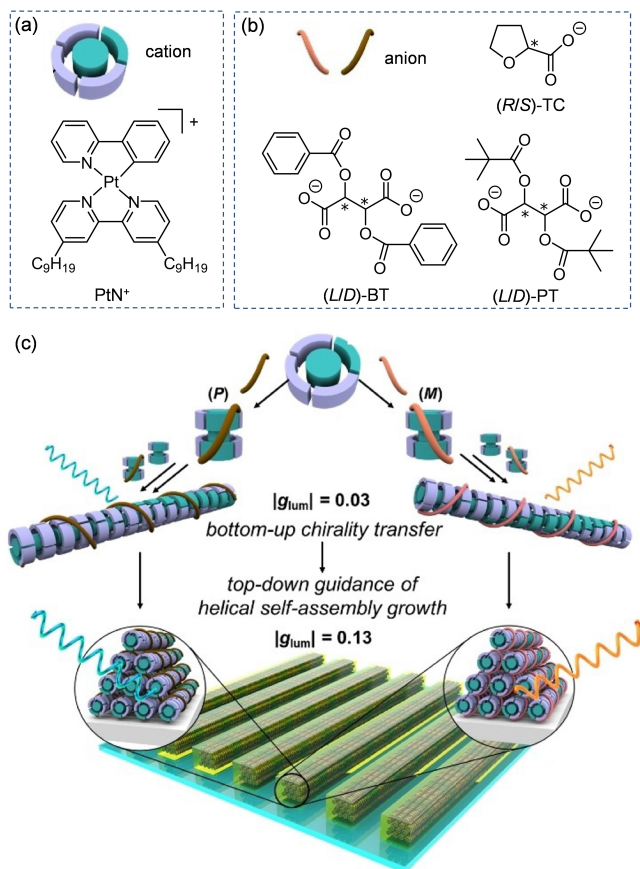


**Figure 4.** (a) Structure of  $\text{PtN}^+$  cation. (b) Structures of carboxylic chiral anions. (c) Schematic representation of the assembly of  $\text{PtN}^+$  cation with (L/D)-BT anion. Reproduced with permission from Ref. [28]. Copyright: 2023, Wiley-VCH.

PT ( $g_{\text{lum}} = 0.023$  and  $-0.026$ , respectively) and (R/S)-TC ( $g_{\text{lum}} = -0.006$  and  $0.001$ , respectively) lead to the decrease of CPL magnitude. This illustrates that the CPL activities are efficiently modulated by the interaction with different chiral anions. The potential  $\pi$ - $\pi$  interaction among the phenyl groups of neighboring (L/D)-BT anion are likely responsible for its favorable interaction with  $\text{PtN}^+$  to give the helical co-assemblies. These researchers further attempted to maximize the chirality amplification by employing the soft-lithographic method of micro-molding in capillaries and the helical self-assemblies of  $\text{PtN}^+((L/D)-\text{BT})$  formed within micro-channels exhibit impressive CPL with  $\Phi$  of  $0.32$  and  $|g_{\text{lum}}|$  of  $0.13$ .

Recently, Zang *et al.* reported the CPL properties of a Au<sup>+</sup> complex  $\text{Au1}^+$  with two acyclic carbene ligands and one chiral ( $\pm$ )-CSA<sup>-</sup> (Figure 5; D/L is used in the paper instead of +/−).<sup>[29]</sup> Single-crystal X-ray analysis indicates that the two N–H groups of the carbene ligands form dual hydrogen bonds with two sulfonate oxygen atoms, which is believed beneficial for the chirality transfer. Four polymorphic crystals of  $\text{Au1}((+)-\text{CSA})$  have been obtained by regulating the condition of crystal growth, showing blue, green, or yellow CPL with  $\Phi$  of  $16\%–95\%$  and  $g_{\text{lum}}$  in the order of  $10^{-4}–10^{-3}$ . The yellow emissions of these crystals are a result of the Au–Au interaction between neighboring molecules. The CPL brightness,  $B_{\text{CPL}}$ , which is used to evaluate

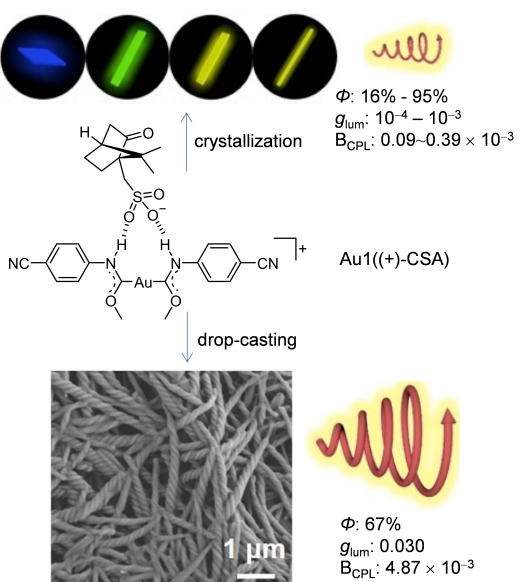


**Figure 5.** The formation of luminescent crystals and helical nanofibres from  $\text{Au1}((+)-\text{CSA})$  with varied CPL properties. Reproduced with permission from Ref. [29]. Copyright: 2023, Wiley-VCH.

the overall CPL performance according to  $B_{\text{CPL}} = \epsilon \times \Phi \times |g_{\text{lum}}|/2$  ( $\epsilon$  is the absorption efficiency),<sup>[30]</sup> is calculated to be  $0.09\text{--}0.39 \times 10^{-3}$  for these crystals. Furthermore,  $\text{Au1}((+)-\text{CSA})$  is assembled into chiral helical nanofibres through a drop-casting method from the solution in mixed solvent of dichloromethane and hexane (9/1), leading to significantly amplified yellow CPL with  $\Phi$  of  $67\%$ ,  $g_{\text{lum}}$  of  $0.030$ , and  $B_{\text{CPL}}$  of  $4.87 \times 10^{-3}$ . When (−)-CSA<sup>-</sup> is used, helical nanofibres with opposite handedness and chiroptical properties are generated. This work, together with the previous example by You and coworkers,<sup>[28]</sup> demonstrate the successful realization of both high  $g_{\text{lum}}$  and  $\Phi$  by the chiral anion-assisted formation of helical assemblies.

## 2.2. Metal Cluster

Metal clusters are relatively stable aggregates composed of several or even thousands of metal atoms connected by metal–metal interactions.<sup>[31]</sup> They have a variety of special physical and chemical characteristics, such as ultra-small size and good biocompatibility. Cluster-based research has become a frontier field in recent years, and chiral metal clusters or metal clusters decorated with chiral functional molecules have attracted considerable attention.<sup>[32]</sup> In comparison with the commonly used methods such as the employment of chiral ligands in clustering processes<sup>[33]</sup> or the enantio-separation by chiral HPLC,<sup>[34]</sup> the chiral counteranion strategy provides a simple way to achieve chiral information in metal clusters.

Axially enantiopure binaphthol (BINOL)-derived phosphate anion is a common chiral counterion inducer in asymmetric chemical synthesis.<sup>[19]</sup> In 2020, this chiral anion was used by Zhao *et al.* to obtain gold chiral metal clusters (Figure 6).<sup>[35]</sup> The enantiomerically pure (R/S)-1,1'-binaphthyl-2,2'-diylphosphate

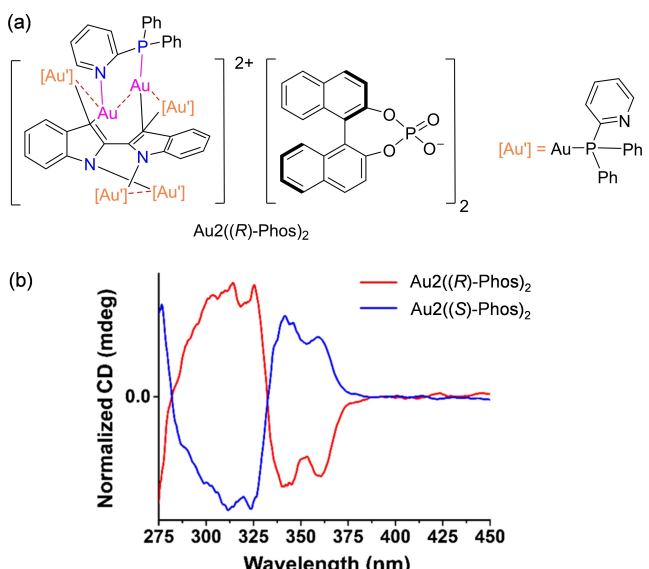


**Figure 6.** Chemical structure of  $\text{Au2}((R)\text{-Phos})_2$  and the CD spectra of  $\text{Au2}((R)\text{-Phos})_2$  and  $\text{Au2}((S)\text{-Phos})_2$  in  $\text{CH}_2\text{Cl}_2$ . Reproduced with permission from Ref. [35]. Copyright: 2020, Chinese Chemical Society.

anions ((R/S)-Phos) were selected as the chiral inducer. For instance, the reaction of the hexa-Au(I) cluster  $\text{Au2}(\text{BF}_4)_2$  containing a biindole core ligand and two tetrafluoroborate anions with the sodium salt of (R/S)-Phos gave chiral  $\text{Au2}((R/S)\text{-Phos})_2$  clusters. The CD spectra of  $\text{Au2}((R/S)\text{-Phos})_2$  display mirror-imaged signals at 341 and 360 nm. Notably, these two peaks are completely absent in the sodium salt of (R/S)-Phos and they reflect the chiroptical property associated with the gold cluster core. This means an efficient chirality transfer occurs from the (R/S)-Phos chiral anion to the gold cluster core. Other examples involving chiral metal clusters will be further discussed below.

### 2.3. Supramolecular Coordination Assembly

Metal-ligand coordination assembly has become a versatile method to prepare multinuclear supramolecules of various shapes and functions.<sup>[36]</sup> The host-guest chemistry of coordination assemblies has been and continues to be a trending topic.<sup>[37]</sup> In particular, the transfer of stereochemical information through guest-to-host noncovalent interactions provides a simple means to endow the coordination assemblies with chiroptical properties. In this context, Clever *et al.* presented a dinuclear Pd(II) coordination cage  $\text{Pd}_2(\text{L1})_4^{4+}$  with four photochromic dithienylethene (DTE)-derived ligands L1 (Figure 7a,b).<sup>[38]</sup> The DTE unit can be present as an open and closed isomer and the intrinsic chirality of the DTE backbones was used as reporters to monitor the inclusion of a chiral guest. When  $\text{Pd}_2(\text{L1})_4^{4+}$  with the open DTE ligands was treated with (+)- or (-)-CSA, CD signals at 330 nm associated with the cage-centered absorption were observed, suggesting an effective chirality transfer from the included chiral CSA guest to the host framework. When the DTE ligands were transformed into closed isomer by UV irradiation, these CD signals disappeared as a result of the ejection of the chiral guest out of the lantern-shaped cage. In addition, the included chiral anion could be completely replaced by a nonchiral guest benzene-1,4-disulfonate (abbreviated as G1), as evidenced by the disappearance of the CD signals at 330 nm.

In the above example, the guest-host chirality transfer of  $\text{Pd}_2(\text{L1})_4^{4+}$  is only effective when the chiral guest is captured inside the cage host. In contrast, Zhang *et al.* recently reported a terpyridine derivative ligand L2-based hexa-Zn(II) cage

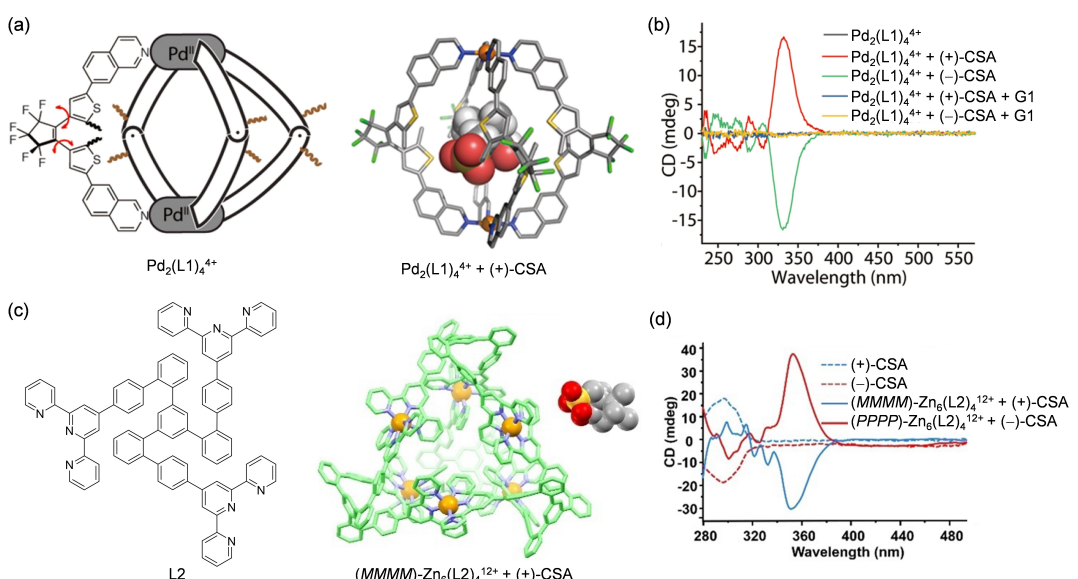


**Figure 7.** (a) Schematic diagram of the structure of the coordination cage  $\text{Pd}_2(\text{L1})_4^{4+}$  and that with an included CSA guest molecule. (b) CD spectra of  $\text{Pd}_2(\text{L1})_4^{4+}$  under different condition. G1 = benzene-1,4-disulfonate. Reproduced with permission from Ref. [38]. Copyright: 2019, American Chemical Society. (c) Structures of ligand L2 and the coordination cage  $(\text{MMMM})\text{-Zn}_6(\text{L2})_4^{12+}$  with a chiral CSA guest molecule outside of the cage. (d) CD spectra of chiral CSA and chiral  $\text{Zn}_6(\text{L2})_4^{12+}$  cage in the presence of corresponding chiral CSA guest. Reproduced with permission from Ref. [39]. Copyright: 2023, Wiley-VCH.

$\text{Zn}_6(\text{L2})_4^{12+}$  with a tetrahedron geometry, in which the presence of a chiral CSA guest outside of the cage could induce effective chirality transfer (Figure 7c,d).<sup>[39]</sup> In ligand L2, the three ortho-substituted terpyridine arms around the central phenyl ring twist either clockwise or anti-clockwise due to the significant space constraint, leading to a *P* or *M* handedness configuration, respectively. When the solution of the racemic mixture of  $\text{Zn}_6(\text{L2})_4^{12+}$  was treated with (+)- or (-)-CSA, the resulting host-guest complex solution showed strong CD signals between 330 and 380 nm, which are ascribed to the chiral (MMMM)- and (PPPP)- $\text{Zn}_6(\text{L2})_4^{12+}$  cage, respectively. The space of this cage was calculated to be too small to accommodate  $\text{CSA}^-$ ; however, this cage could provide peripheral binding pockets to interact with CSA guest molecules. In this sense, efficient chirality transfer occurred from the chiral  $\text{CSA}^-$  outside of the  $\text{Zn}_6(\text{L2})_4^{12+}$  cage to the supramolecular framework, leading to the appearance of the CD signals between 330 and 380 nm.

#### 2.4. Metal-Organic Framework and Related Material

MOFs are a unique class of porous crystalline materials comprised of metal cations or metal clusters coordinated with organic ligands.<sup>[40]</sup> Because of their high porosity, high specific surface area, good thermal stability, and modified chemical properties, MOFs have been applied in a wide range disciplines including biological sciences, gas separation and absorption, photo- and electrocatalysis, luminescence, sensing, and so on.<sup>[41]</sup> Among them, the preparation and applications of luminescent MOFs has been intensively investigated.<sup>[42]</sup> The luminescence of MOFs can arise from the conjugated organic ligands, metal components or clusters, or the charge transfer among different components. The combination of chirality and luminescent MOFs affords chiral luminescent materials with potential applications in enantioselective recognition, asymmetric catalysis, light-emitting devices, among others.<sup>[43]</sup>

Typically, the chirality of chiral MOFs can be derived by the chirality transmission from chiral building blocks<sup>[44]</sup> or the structural chirality formed from achiral building blocks by spontaneous resolution or chiral induction.<sup>[45]</sup> In this context, chiral anions stand out as an easily accessible chiral inducer by potent interactions with the host framework. For instance, Wu *et al.* reported a two-dimensional (2D) layered network  $\text{Zn}(\text{II})$  MOF with disordered  $\text{ClO}_4^-$  filling the spaces between neighboring layers.<sup>[46]</sup> By substituting  $\text{ClO}_4^-$  partially with the chiral guest (*L/D*)-pyroglutamate anion, enantiomeric MOFs were produced showing CD signals associated with the framework structure. Zhang *et al.* utilized (*R*)-5-(1-carboxyethoxy)isophthalic acid as a chiral template to obtain a homochiral  $\text{Zn}(\text{II})$  MOFs featuring a GIS-type framework with two types of helical chains and nanochannels filled with the chiral anions.<sup>[47]</sup> Li *et al.* reported the reaction of  $\text{Cu}^{2+}$  with an achiral 4,2':6',4''-terpyridine derivative ligand, accompanied by spontaneous resolution, to give a type of three-dimensional (3D) chiral  $\text{Cu}(\text{II})$  coordination polymers as conglomerate.<sup>[48]</sup> In addition, in the presence of chiral  $\text{CSA}^-$ , enantioenriched chiral  $\text{Cu}(\text{II})$  coordination polymers was obtained, with the chiral anions being included into the cavity of the 3D polymers. In these works, the efficient chirality transfer from chiral anions is supported by the observation of CD signals associated with the framework structures. However, no CPL property is reported from these chiral coordination materials.

Recently, Zang *et al.* constructed chiral metal cluster-based MOFs showing strong CPL emissions through the chiral anionic strategy (Figure 8).<sup>[49]</sup> They first prepared chiral enantiomeric single crystals  $[\text{Ag}_{12}(\text{S'Pr})_6((+/-)\text{-CSA})_6(\text{MeOH})_4]_n$ , in which the  $\text{Ag}_{12}$ -nanoclusters are linked by chiral  $\text{CSA}^-$ . These crystals were used as the basic secondary building units for the following coordination assembly with a pyridine-terminated anthracene derivative or ion pair-directed assembly with the protonated pyridine derivative. The coordination assembly affords crystalline MOF materials with a  $\Phi$  of 50.3% and a superb CPL signal with  $|g_{\text{lum}}|$  up to 0.012. In comparison, the composite material

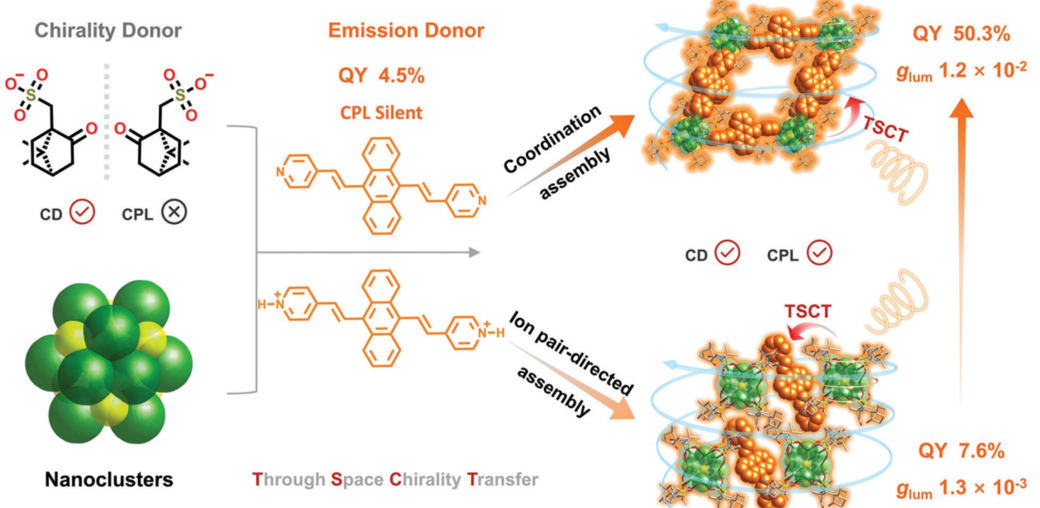


**Figure 8.** Schematically illustrating a chiral reticular self-assembly with a chirality donor, nanoclusters and an organic luminophore.  $\text{QY} = \Phi$ . Reproduced with permission from Ref. [49]. Copyright: 2023, Wiley-VCH.

obtained after the ion pair-directed assembly shows inferior luminescence and CPL performance. Crystallographic analyses and DFT calculations suggest that the quasi-parallel arrangement of the emitting linkers in MOF materials leads to a large angle between the electric and magnetic transition dipole moments and thus boosts the CPL performance.

### 3. Summary and Outlook

Chiroptical materials with CD or CPL activity have received intensive attention in the past decades. Among them, chiral metal-organic coordination materials feature varied modes of assembly and rich photophysical properties, representing a promising candidate for a wide range of optoelectronic applications. We summarize in this article the recent progress in inducing chirality in ionic coordination materials through the chiral anion strategy. Compared to the commonly used synthetic methods including the transformation from intrinsically chiral building blocks or chiral symmetry breaking of achiral materials, the chiral anion strategy offers a simple and economical method to endow materials with chiroptical activities by chirality transfer. This method has been successfully implemented in coordination materials including small-molecular metal complexes, metal clusters, coordination assemblies, and MOFs. In addition to photoinduced CPLs, the realization of CPELs using the chiral anion strategy has also been demonstrated.

Considering the recent intensive interest in chiral luminescent materials and the simplicity of the chiral anion strategy in inducing chiroptical properties, this method is slated to attract increasing attention once four principal deficits of the research area are addressed. Firstly, the exploration of the effect of chiral anion species has been only superficial. To date, mostly chiral  $\text{CSA}^-$  anions have been utilized and the explorations of other chiral anions such as carboxylic or phosphoric anions were only peripheral. Ionic materials containing  $\text{CSA}^-$  sometimes suffer from the hygroscopic issue, making them unstable in humid conditions. The use of other chiral anions may alleviate this problem. In addition, the relationship between the structures of chiral anions and chiroptical properties remains an interesting topic to be investigated in the future. To date, only limited efforts have been devoted to this aspect.<sup>[28]</sup> Secondly, the  $g_{\text{lum}}$  values of the induced CPLs of these chiral anion-containing coordination materials are in general low ( $<0.1$ ). These values are still far from satisfactory compared to the theoretical value of  $\pm 2$ , limiting their promise practical applications, but the development of new chiral anions or new assembly methods may improve the overall CPL performance of these materials. Thirdly, the scope of the coordination materials remains to be expanded. To date, this method has been implemented in Ru(II), Ir(III), Pt(II), Au(I), Pd(II), Zn(II) Cu(II) complexes and assemblies. Whether this chiral anion method is effective in other metal complexes such as lanthanide and Cr(III) complexes awaits to be investigated. The latter two complexes have been known to demonstrate CPLs with large  $g_{\text{lum}}$  values due to their unique magnetic and electronic properties.<sup>[21]</sup> Fourthly, a mechanistic understanding of the chirality transfer between chiral anions and complexes is urgently

needed. Considering the dynamic nature of counter anions, which is different from covalent chiral systems, the investigation on the underlying chirality transfer process would be rather difficult. This may require the assistance of advanced characterization techniques with high time- and space-resolutions. In addition, the dynamic cation-anion noncovalent interaction can be utilized to develop stimuli-responsive chiroptical materials.

Though only coordination materials are discussed in this concept article, the chiral anion strategy should also be applicable to other ionic luminophores, e.g. organic or organic-inorganic hybrid materials. We hope that this method will provide a general strategy for the design and synthesis of chiroptical materials, which would eventually promote the applications of these materials.

### Acknowledgements

We acknowledge the funding support from the National Key R&D Program of China (2023YFE0125200 and 2022YFA1204401) and the National Natural Science Foundation of China (grant 21925112, 22090021 and 22305251). Z.-Q.L. is grateful to the support of the BMS Junior Fellow of BNLMS. S.B. gratefully acknowledges support by the US NSF (CHE-2102460).

### Conflict of Interests

The authors declare no conflict of interest.

### Data Availability Statement

Data sharing is not applicable to this article as no new data were created or analyzed in this study.

**Keywords:** circularly polarized luminescence • chiral anion • photofunctional metal complexes • coordination assembly • chiral materials

- [1] a) Y. Wang, J. Xu, Y. Wang, H. Chen, *Chem. Soc. Rev.* **2013**, *42*, 2930–2962; b) G. Albano, G. Pescitelli, L. Di Bari, *Chem. Rev.* **2020**, *120*, 10145–10243; c) G. Ouyang, M. Liu, *Chin. J. Struct. Chem.* **2023**, *42*, 100007.
- [2] a) C. Train, R. Gheorghe, V. Krstic, L.-M. Chamoreau, N. S. Ovanesyan, G. L. J. A. Rikken, M. Gruselle, M. Verdaguer, *Nat. Mater.* **2008**, *7*, 729–734; b) H. Zhu, J. Yi, M.-Y. Li, J. Xiao, L. Zhang, C.-W. Yang, R. A. Kaindl, L.-J. Li, Y. Wang, X. Zhang, *Science* **2018**, *359*, 579–582; c) Z.-L. Gong, X. Zhu, Z. Zhou, S.-W. Zhang, D. Yang, B. Zhao, Y.-P. Zhang, J. Deng, Y. Cheng, Y.-X. Zheng, S.-Q. Zang, H. Kuang, P. Duan, M. Yuan, C.-F. Chen, Y.-S. Zhao, Y.-W. Zhong, B.-Z. Tang, M. Liu, *Sci. China Chem.* **2021**, *64*, 2060–2104; d) A. Ying, L. Zhan, Y. Tan, X. Cao, C. Yang, S. Gong, *Sci. China Chem.* **2023**, *66*, 2274–2282; e) B. Ma, A. Bianco, *Nat. Rev. Mater.* **2023**, *8*, 403–413; f) F. R. Tarrío, E. Quiñoá, G. Fernández, F. Freire, *Nat. Commun.* **2023**, *14*, 3348.
- [3] G. Namba, Y. Mimura, Y. Imai, R. Inoue, Y. Morisaki, *Chem. Eur. J.* **2020**, *26*, 14871–14877.
- [4] S.-P. Wan, H.-Y. Lu, M. Li, C.-F. Chen, *J. Photochem. Photobiol. C* **2022**, *50*, 100500.
- [5] a) T. Mori, *Chem. Rev.* **2021**, *121*, 2373–2412; b) M. Cei, L. D. Bari, F. Zinna, *Chirality* **2023**, *35*, 192–210.

[6] a) J. Liu, S. Mukherjee, F. Wang, R. A. Fischer, J. Zhang, *Chem. Soc. Rev.* **2021**, *50*, 5706–5745; b) Y. Wang, X. Zhao, N. Qu, J. Gu, *Org. Electron.* **2023**, *122*, 106902; c) X. Niu, R. Zhao, S. Yan, Z. Pang, H. Li, X. Yang, K. Wang, *Small* **2023**, *19*, 2303059; d) Y. Sang, M. Liu, *Chem. Sci.* **2022**, *13*, 633–656.

[7] a) W. Ma, C. Hao, M. Sun, L. Xu, C. Xu, H. Kuang, *Mater. Horiz.* **2018**, *5*, 141–161; b) J. L. Greenfield, J. Wade, J. R. Brandt, X. Shi, T. J. Penfold, M. J. Fuchter, *Chem. Sci.* **2021**, *12*, 8589–8602; c) G. Zhang, Y. Bao, M. Pan, N. Wang, X. Cheng, W. Zhang, *Sci. China Chem.* **2023**, *66*, 1169–1178; d) Y. Liu, A. Hao, P. Xing, *Sci. China Chem.* **2023**, *66*, 2130–2140.

[8] a) H. Zhong, B. Zhao, J. Deng, *Adv. Opt. Mater.* **2023**, *11*, 2202787; b) Y. Wu, M. Li, Z. Zheng, Z.-Q. Yu, W.-H. Zhu, *J. Am. Chem. Soc.* **2023**, *145*, 12951–12966.

[9] Y. Deng, M. Wang, Y. Zhuang, S. Liu, W. Huang, Q. Zhao, *Light-Sci. Appl.* **2021**, *10*, 76.

[10] a) Y. Sang, D. Yang, P. Duan, M. Liu, *Chem. Sci.* **2019**, *10*, 2718–2724; b) X. Ye, J. Cui, B. Li, N. Li, R. Wang, Z. Yan, J. Tan, J. Zhang, X. Wan, *Nat. Commun.* **2019**, *10*, 1964; c) C.-Y. Ding, Y.-W. Zhong, J. Yao, *CCS Chem.* **2024**, doi: 10.31635/ccschem.024.202403864.

[11] a) C. Yang, W. Chen, X. Zhu, X. Song, M. Liu, *J. Phys. Chem. Lett.* **2021**, *12*, 7491–7496; b) S. Fa, T. Tomita, K. Wada, K. Yasuhara, S. Ohtani, K. Kato, M. Gon, K. Tanaka, T. Kakuta, T. Yamagishib, T. Ogoshi, *Chem. Sci.* **2022**, *13*, 5846–5853.

[12] a) F. Nie, D. Yan, *Angew. Chem. Int. Ed.* **2023**, *62*, e202302751; b) X. Dou, N. Mehewish, C. Zhao, J. Liu, C. Xing, C. Feng, *Acc. Chem. Res.* **2020**, *53*, 852–862.

[13] a) J. Han, D. Yang, X. Jin, Y. Jiang, M. Liu, P. Duan, *Angew. Chem. Int. Ed.* **2019**, *58*, 7013–7019; b) B. Liu, J. Gao, A. Hao, P. Xing, *Angew. Chem. Int. Ed.* **2023**, *62*, e202305135.

[14] a) K. Watanabe, H. Iida, K. Akagi, *Adv. Mater.* **2012**, *24*, 6451–6456; b) T. Goto, Y. Okazaki, M. Ueki, Y. Kuwahara, M. Takafuji, R. Oda, H. Ihara, *Angew. Chem. Int. Ed.* **2017**, *56*, 2989–2993.

[15] Y. Zhang, H. Li, Z. Geng, W.-H. Zheng, Y. Quan, Y. Cheng, *ACS Nano* **2022**, *16*, 3173–3181.

[16] a) Z.-L. Gong, Z.-Q. Li, Y.-W. Zhong, *Aggregate* **2022**, *3*, e177; b) Y.-P. Zhang, Y.-X. Zheng, *Dalton Trans.* **2022**, *51*, 9966–9970; c) J. Gong, X. Zhang, *Coord. Chem. Rev.* **2022**, *453*, 214329; d) X.-Y. Luo, M. Pan, *Coord. Chem. Rev.* **2022**, *468*, 214640.

[17] a) J. L. Lunkley, D. Shirotani, K. Yamanari, S. Kaizaki, G. Muller, *J. Am. Chem. Soc.* **2008**, *130*, 13814–13815; b) Y. Kitagawa, M. Tsurui, Y. Hasegawa, *ACS Omega* **2020**, *5*, 3786–3791.

[18] a) V. Yam, V. Au, S. Leung, *Chem. Rev.* **2015**, *115*, 7589–7728; b) R. Li, F.-F. Xu, Z.-L. Gong, Y.-W. Zhong, *Inorg. Chem. Front.* **2020**, *7*, 3258–3281.

[19] a) M. Mahlau, B. List, *Angew. Chem. Int. Ed.* **2013**, *52*, 518–533; b) Z. Zhang, V. Smal, P. Retailleau, A. Voituriez, G. Frison, A. Marinetti, X. Guinchard, *J. Am. Chem. Soc.* **2020**, *142*, 3797–3805; c) A. Franchino, A. Marti, A. M. Echavarren, *J. Am. Chem. Soc.* **2022**, *144*, 3497–3509.

[20] a) Z.-Q. Li, Z.-L. Gong, J.-Y. Shao, J. Yao, Y.-W. Zhong, *Angew. Chem. Int. Ed.* **2021**, *60*, 14595–14600; b) L. Meng, Z.-Q. Li, K. Tang, J.-Y. Shao, Z. Chen, Y.-W. Zhong, *J. Mater. Chem. C* **2023**, *11*, 676–684.

[21] a) B. Doistau, J.-R. Jiménez, C. Piguet, *Front. Chem.* **2020**, *8*, 555; b) M. Poncet, A. Benchohra, J.-R. Jiménez, C. Piguet, *ChemPhotoChem* **2021**, *5*, 880–892.

[22] a) M. S. Lowry, W. R. Hudson, R. A. Pascal, S. Bernhard, *J. Am. Chem. Soc.* **2004**, *126*, 14129–14135; b) C. Schaffner-Hamann, A. Zelewsky, A. Barbieri, F. Barigelli, G. Muller, J. P. Riehl, A. Neels, *J. Am. Chem. Soc.* **2004**, *126*, 9339–9348; c) K. D. Oyler, F. J. Coughlin, S. Bernhard, *J. Am. Chem. Soc.* **2007**, *129*, 210–217; d) F. J. Coughlin, M. S. Westrol, K. D. Oyler, N. Byrne, C. Kraml, E. Zysman-Colman, M. S. Lowry, S. Bernhard, *Inorg. Chem.* **2008**, *47*, 2039–2048; e) T.-Y. Li, Y.-M. Jing, X. Liu, Y. Zhao, L. Shi, Z. Tang, Y.-X. Zheng, J.-L. Zuo, *Sci. Rep.* **2015**, *5*, 14912.

[23] a) O. Chepelin, J. Ujma, X. Wu, A. M. Z. Slawin, M. B. Pitak, S. J. Coles, J. Michel, A. C. Jones, P. E. Barran, P. J. Lusby, *J. Am. Chem. Soc.* **2012**, *134*, 19334–19337; b) C. Fu, M. Wenzel, E. Treutlein, K. Harms, E. Meggers, *Inorg. Chem.* **2012**, *51*, 10004–10011; c) Y.-P. Zhang, Y.-X. Zheng, *Dalton Trans.* **2022**, *51*, 9966–9970.

[24] Z.-Q. Li, Z.-L. Gong, T. Liang, S. Bernhard, Y.-W. Zhong, J. Yao, *Sci. China Chem.* **2023**, *66*, 2892–2902.

[25] Z.-Q. Li, Y.-D. Wang, J.-Y. Shao, Z.-Y. Zhou, Z.-L. Gong, C. Zhang, J. Yao, Y.-W. Zhong, *Angew. Chem. Int. Ed.* **2023**, *62*, e202302160.

[26] a) J. R. Brandt, X. Wang, Y. Yang, A. J. Campbell, M. J. Fuchter, *J. Am. Chem. Soc.* **2016**, *138*, 9743–9746; b) F. Zinna, M. Pasini, F. Galeotti, C. Botta, L. Di Bari, U. Giovanella, *Adv. Funct. Mater.* **2017**, *27*, 1603719; c) G. Lu, Z.-G. Wu, R. Wu, X. Cao, L. Zhou, Y.-X. Zheng, C. Yang, *Adv. Funct. Mater.* **2021**, *31*, 2102898.

[27] a) W. Shang, X. Zhu, Y. Jiang, J. Cui, K. Liu, T. Li, M. Liu, *Angew. Chem. Int. Ed.* **2022**, *61*, e202210604; b) L. Hu, K. Li, W. Shang, X. Zhu, M. Liu, *Angew. Chem. Int. Ed.* **2020**, *59*, 4953–4958.

[28] G. Park, D. Y. Jeong, S. Y. Yu, J. J. Park, J. H. Kim, H. Yang, Y. You, *Angew. Chem. Int. Ed.* **2023**, *62*, e202309762.

[29] Y.-J. Liu, Y. Liu, S.-Q. Zang, *Angew. Chem. Int. Ed.* **2023**, *62*, e202311572.

[30] L. Arrico, L. Di Bari, F. Zinna, *Chem. Eur. J.* **2021**, *27*, 2920–2934.

[31] a) M.-M. Zhang, X.-Y. Dong, Y.-J. Wang, S.-Q. Zang, T. C. W. Mak, *Coord. Chem. Rev.* **2022**, *453*, 214315; b) B.-W. Zhou, S. Zhang, L. Zhao, *Mater. Chem. Front.* **2023**, *7*, 6389–6410.

[32] a) M.-M. Zhang, X.-Y. Dong, Z.-Y. Wang, X.-M. Luo, J.-H. Huang, S.-Q. Zang, T. C. W. Mak, *J. Am. Chem. Soc.* **2021**, *143*, 6048–6053; b) X. Jing, F. Fu, R. Wang, X. Xin, L. Qin, H. Lv, G.-Y. Yang, *ACS Nano* **2022**, *16*, 15188–15196.

[33] a) C. Liu, Y. Zhao, T.-S. Zhang, C.-B. Tao, W. Fei, S. Zhang, M.-B. Li, *Nat. Commun.* **2023**, *14*, 3730; b) P. Luo, X.-J. Zhai, S. Bai, Y.-B. Si, X.-Y. Dong, Y.-F. Han, S.-Q. Zang, *Angew. Chem. Int. Ed.* **2023**, *62*, e202219017.

[34] a) I. Dolamic, S. Knoppe, A. Dass, T. Bürgi, *Nat. Commun.* **2012**, *3*, 798; b) S. Knoppe, T. Bürgi, *Acc. Chem. Res.* **2014**, *47*, 1318–1326.

[35] K. Xiao, Y. Xue, B. Yang, L. Zhao, *CCS Chem.* **2020**, *3*, 555–565.

[36] a) S. Chakraborty, G. R. Newkome, *Chem. Soc. Rev.* **2018**, *47*, 3991–4016; b) W.-X. Gao, H.-J. Feng, B.-B. Guo, Y. Lu, G.-X. Jin, *Chem. Rev.* **2020**, *120*, 6288–6325; c) J. Liu, J. Zhang, L. Zhang, Y. Wang, H. Wei, Y. Shen, J. Min, X. Rong, W. Qi, R. Su, Z. He, *Sci. China Chem.* **2023**, *66*, 228–241; d) C. Li, J.-M. Xi, Z.-Z. Lu, R. Zhang, L. Huang, *Chinese J. Inorg. Chem.* **2023**, *39*, 2425–2431; e) Y.-M. Bao, Y.-H. Chen, Y.-Y. Xing, J.-Y. Zhang, W. Deng, *Chinese J. Inorg. Chem.* **2023**, *39*, 993–1004.

[37] L.-J. Chen, H.-B. Yang, M. Shionoya, *Chem. Soc. Rev.* **2017**, *46*, 2555–2576.

[38] R.-J. Li, J. J. Holstein, W. G. Hiller, J. Andréasson, G. H. Clever, *J. Am. Chem. Soc.* **2019**, *141*, 2097–2103.

[39] Q. Bai, Y.-M. Guan, T. Wu, Y. Liu, Z. Zhai, Q. Long, Z. Jiang, P. Su, T.-Z. Xie, P. Wang, Z. Zhang, *Angew. Chem. Int. Ed.* **2023**, *62*, e202309027.

[40] a) D. J. Tranchemontagne, J. L. Mendoza-Cortés, M. O’Keeffe, O. M. Yaghi, *Chem. Soc. Rev.* **2009**, *38*, 1257–1283; b) Y. Xu, Q. Li, H. Xue, H. Pang, *Coord. Chem. Rev.* **2018**, *376*, 292–318.

[41] a) S. Navalón, A. Dhakshinamoorthy, M. Álvaro, B. Ferrer, H. García, *Chem. Rev.* **2023**, *123*, 445–490; b) A. M. Rice, C. R. Martin, V. A. Galitskiy, A. A. Berseneva, G. A. Leith, N. B. Shustova, *Chem. Rev.* **2020**, *120*, 8790–8813; c) H. Yang, L. Xue, X. Yang, H. Xu, J. Gao, *Chin. J. Struct. Chem.* **2023**, *42*, 100034; d) K. Wu, X.-Y. Liu, P.-W. Cheng, M. Xie, W. Lu, D. Li, *Sci. China Chem.* **2023**, *66*, 1634–1653.

[42] a) Z. Hu, B. J. Deibert, J. Li, *Chem. Soc. Rev.* **2014**, *43*, 5815; b) J. Rocha, L. D. Carlos, F. A. A. Paz, D. Ananias, *Chem. Soc. Rev.* **2011**, *40*, 926–940; c) P.-D. Liu, A.-G. Liu, P.-M. Wang, Y. Chen, B. Li, *Chin. J. Struct. Chem.* **2023**, *42*, 100001; d) Y. Zhao, H. Zeng, X.-W. Zhu, W. Lu, D. Li, *Chem. Soc. Rev.* **2021**, *50*, 4484–4513.

[43] a) Q. Cheng, Q. Ma, H. Pei, H. Liang, X. Zhang, X. Jin, N. Liu, R. Guo, Z. Mo, *Coord. Chem. Rev.* **2023**, *484*, 215120; b) C. Zhang, Z.-P. Yan, X.-Y. Dong, Z. Han, S. Li, T. Fu, Y.-Y. Zhi, Y.-X. Zheng, Y.-Y. Niu, S.-Q. Zang, *Adv. Mater.* **2020**, *32*, 2002914.

[44] a) W. Gong, Z. Chen, J. Dong, Y. Liu, Y. Cui, *Chem. Rev.* **2022**, *122*, 9078–9144; b) L. A. Hall, D. M. Alessandro, G. Lakhwani, *Chem. Soc. Rev.* **2023**, *52*, 3567–3590; c) K. Berijani, L.-M. Chang, Z.-G. Gu, *Coord. Chem. Rev.* **2023**, *474*, 214852.

[45] D. Wu, K. Zhou, J. Tian, C. Liu, J. Tian, F. Jiang, D. Yuan, J. Zhang, Q. Chen, M. Hong, *Angew. Chem. Int. Ed.* **2021**, *60*, 3087–3094.

[46] Y. Wen, T. Sheng, S. Hu, X. Ma, C. Tan, Y. Wang, Z. Sun, Z. Xue, X. Wu, *Chem. Commun.* **2013**, *49*, 10644–10646.

[47] Z.-X. Xu, Y.-L. Ma, J. Zhang, *Chem. Commun.* **2016**, *52*, 1923–1925.

[48] T. Zuo, D. Luo, Y.-L. Huang, Y. Li, X.-P. Zhou, D. Li, *Chem. Eur. J.* **2020**, *26*, 1936–1940.

[49] J.-Y. Wang, Y. Si, X.-M. Luo, Z.-Y. Wang, X.-Y. Dong, P. Luo, C. Zhang, Duan, S.-Q. Zang, *Adv. Sci.* **2023**, *10*, 2207660.

Manuscript received: February 19, 2024

Accepted manuscript online: March 12, 2024

Version of record online: April 5, 2024